

UCD-97-24	
DOE-ER40757-107	
UTEXAS-HEP-97-21	
OITS-639	
OSURN-331	

Multilepton signatures of gauge mediated SUSY breaking at LEPII

Kingman Cheung^{1,2,3}, Duane A. Dicus^{1,2},
B. Dutta⁴, and S. Nandi⁵

¹ *Center for Particle Physics, University of Texas, Austin, TX 78712*

² *Department of Physics, University of Texas, Austin, TX 78712*

³ *Department of Physics, University of California at Davis, Davis, CA 95616*

⁴ *Institute of Theoretical Science, University of Oregon, Eugene, OR 97403*

⁵ *Department of Physics, Oklahoma State University, Stillwater, OK 74078*

(October, 1997)

Abstract

In the framework of gauge-mediated supersymmetry breaking models pair production of the lightest neutralinos, scalar leptons, or charginos at LEPII gives rise to interesting signals involving multilepton final states and missing energy. In the parameter space where the scalar tau, $\tilde{\tau}_1$, is the next-to-lightest supersymmetric particle, we identify three interesting regions, which give rise to distinctly different final states: (i) 2 τ -leptons plus missing energy, (ii) 4 charged leptons plus missing energy where in some regions all four are τ -leptons, or (iii) six charged leptons, of which four are τ -leptons and the other

two are electrons or muons, plus missing energy. We study in detail the size of these regions in the parameter space of gauge-mediated models and give cross section contours in these regions for various LEPII energies. We also discuss the possibility of chargino-pair production at LEPII. In addition, we point out an important effect of beam polarization on the production cross sections, which can help distinguishing the gauge-mediated models from the usual supergravity models.

PACS numbers: 11.30.Pb 12.60.Jv 14.80.Ly

I. INTRODUCTION

Supersymmetry is usually assumed to be broken in a hidden sector and then communicated to the observable sector, but how this communication happens is an area of active research. Most commonly, this communication is via gravity, the result of which is that the soft terms are introduced at around the Planck scale ($\sim 10^{18}$ GeV). This mode of communication, however, has the problem of uncontrolled flavor violation, which needs to be harnessed by some symmetry. Further, if these terms are introduced at the Planck scale or at the string scale, one needs a definite unification group from the GUT scale ($\sim 2 \times 10^{16}$ GeV) up to the Planck scale, because in the minimal supersymmetric standard Model (MSSM) the couplings unify at the GUT scale. Consequently, the radiative corrections to the fields depend on the particular choice of the unifying group. Recently, another class of models has become very popular. In these models communication takes place via gauge interactions which have the standard model (SM) gauge symmetry [1] or a new gauge symmetry [2]. These models are naturally devoid of flavor violation. The soft terms are introduced at a scale around 100 TeV. Comparing with the supergravity-motivated models, gauge-mediated models have fewer parameters because the coefficients of the trilinear terms in the potential (A terms) are zero at the boundary. We will concentrate on this type of models in this paper.

The gravitino is always the LSP in these gauge-mediated supersymmetry breaking (GMSB) models. For the NLSP spot there is a competition between the lighter scalar tau (stau) $\tilde{\tau}_1$ and the lightest neutralino $\tilde{\chi}_1^0$. The winner is decided by the input parameters. Signals from the production of SUSY particles can distinguish which is the NLSP. The phenomenology when the lightest neutralino is the NLSP and the resulting signals of hard photons plus missing energy (due to the gravitinos) have been discussed extensively for the Tevatron and for LEPII [3–15]. If the scalar tau $\tilde{\tau}_1$ is the NLSP its decay to a τ -lepton and a gravitino gives rise to a signature of extra τ -leptons plus missing energy, without any hard photons. The production of neutralinos, scalar electrons (selectrons), scalar muons

(smuons), and staus as well as their signatures have been discussed in the literature by us and others [16–20]. In this paper, we elaborate on the processes specific to LEPII where the stau is the NLSP and determine the regions in the parameter space that can be probed by LEPII.

For a beam energy $E_{\text{beam}} = E_{CM}/2$ at LEPII the parameter space can be divided into three distinct regions:

- Region I: $E_{\text{beam}} > m_{\tilde{\chi}_1^0} > m_{\tilde{e}_1} > m_{\tilde{\tau}_1}$, where the lightest selectron \tilde{e}_1 is usually the right-handed one \tilde{e}_R . In this region, the final state will be $4e$, 4μ , 4τ , $2e2\mu$, $2e2\tau$, or $2\mu2\tau$ plus missing energy.
- Region II: $E_{\text{beam}} > m_{\tilde{e}_1} > m_{\tilde{\chi}_1^0} > m_{\tilde{\tau}_1}$. Here the signals are 4τ or 6 charged leptons plus missing energy.
- Region III: $m_{\tilde{e}_1} > E_{\text{beam}} > m_{\tilde{\chi}_1^0} > m_{\tilde{\tau}_1}$. In this region, the signal will be 4τ plus missing energy.

The smuon mass is assumed to be equal to the selectron mass. In each of these regions a pair of staus can be directly produced but it gives a signal of only two τ -leptons plus missing energy, which not only has a smaller cross section but also suffers from WW background.

Our objective is to make a detailed study of the GMSB parameter space to see how probable these regions are and to investigate the corresponding signals. The organization of the paper is as follows. In section II we discuss the GMSB parameter space and how we calculate the sparticle mass spectrum and how to identify the regions in which $\tilde{\tau}_1$ is the NLSP. In section III we discuss the production processes contributing to the signals and the final states in the regions I, II, and III. In section IV, we give our results and describe in detail the signals in regions I, II, and III. Section V contains a brief discussion on the prospect of chargino-pair production at LEPII. In section VI, we discuss the effect of beam polarization. Section VII contains our conclusions.

II. GMSB PARAMETER SPACE WITH $\tilde{\tau}_1$ AS NLSP

In GMSB models the sparticle masses depend on five parameters: $M, \Lambda, n, \tan \beta$, and $\text{sign}(\mu)$. M is the messenger scale, $M = \lambda \langle s \rangle$, where $\langle s \rangle$ is the VEV of the scalar component of superfield in the hidden sector and λ is the Yukawa coupling. The parameter Λ is equal to $\langle F_s \rangle / \langle s \rangle$, where $\langle F_s \rangle$ is the VEV of the auxiliary component of the superfield. F_s can be of order of the intrinsic SUSY breaking scale F . In GMSB models, Λ is taken to be around 100 TeV so that the colored superpartners have masses around 1 TeV or less. The parameter n is fixed by the choice of the messenger sector. The messenger-sector representations should be vector-like (for example, $5 + \bar{5}$ of $SU(5)$, $10 + \bar{10}$ of $SU(5)$ or $16 + \bar{16}$ of $SO(10)$) so that their masses are well above the electroweak scale. They are also chosen to transform as a GUT multiplet in order not to affect the gauge coupling unification in MSSM. These facts restrict $n(5 + \bar{5}) \leq 4$, or $n(10 + \bar{10}) \leq 1$ in $SU(5)$, and $n(16 + \bar{16}) \leq 1$ in an $SO(10)$ GUT for the messenger sector (one $10 + \bar{10}$ pair corresponds to $n(5 + \bar{5})=3$). The parameter $\tan \beta$ is the usual ratio of the up (H_u) and down (H_d) type Higgs VEVs. The parameter μ is the coefficient in the bilinear term, $\mu H_u H_d$, in the superpotential while another parameter B is defined to be the coefficient in the bilinear term, $B \mu H_u H_d$, in the potential. In general, μ and B depend on the details of the SUSY breaking in the hidden sector. We demand that the electroweak symmetry is broken radiatively, which determines μ^2 and B in terms of other parameters of the theory. Thus we are left with five independent parameters, $M, \Lambda, n, \tan \beta$ and $\text{sign}(\mu)$. The soft SUSY breaking gaugino and the scalar masses at the messenger scale M are given by [21]

$$\tilde{M}_i(M) = n g \left(\frac{\Lambda}{M} \right) \frac{\alpha_i(M)}{4\pi} \Lambda$$

and

$$\tilde{m}^2(M) = 2 n f \left(\frac{\Lambda}{M} \right) \sum_{i=1}^3 k_i C_i \left(\frac{\alpha_i(M)}{4\pi} \right)^2 \Lambda^2$$

where α_i ($i = 1 - 3$) are the three SM gauge couplings and $k_i = 1, 1, 3/5$ for $SU(3)$, $SU(2)$, and $U(1)$, respectively. The C_i are zero for gauge singlets, and $4/3, 3/4$, and $(Y/2)^2$ for the

fundamental representations of $SU(3)$ and $SU(2)$ and $U(1)_Y$ respectively (with Y defined by $Q = I_3 + Y/2$). Here n corresponds to $n(5 + \bar{5})$. $g(x)$ and $f(x)$ are messenger scale threshold functions with $x = \Lambda/M$ [21].

We calculate the SUSY mass spectrum using the appropriate RGE equations [22] with the boundary conditions given by the equations above and vary the five free parameters. For the messenger sector, we choose $5 + \bar{5}$ of $SU(5)$, and varied $n(5 + \bar{5})$ from 1 to 4. In addition to the current experimental bounds on the superpartner masses, the rate for $b \rightarrow s\gamma$ restricts $\mu < 0$ [7,8,23]. In the absence of late inflation, cosmological constraints put an upper bound on the gravitino mass of about 10^4 eV [24], which restricts $M/\Lambda = 1.1 - 10^4$. It is found that for $n = 1$ and $\tan \beta \lesssim 25$ the lightest neutralino $\tilde{\chi}_1^0$ is the NLSP [7,9]. As $\tan \beta$ increases further, $\tilde{\tau}_1$ becomes the NLSP. For $n \geq 2$, $\tilde{\tau}_1$ is the NLSP even for low values of $\tan \beta$ ($\tan \beta \gtrsim 2$), and for $n \geq 3$ $\tilde{\tau}_1$ is naturally the NLSP for most of the parameter space.

III. COLLIDER SIGNALS WITH $\tilde{\tau}_1$ AS THE NLSP

In this section, we discuss the various processes that could give rise to observable signals at LEPII. We divide the parameter space into the three regions based on the mass hierarchies of the superpartners. The final states can be different in these three regions. By searching for the signals of regions I, II, and III the LEPII experiments should find SUSY or be able to exclude parts or all of these regions in the parameter space.

In region I ($E_{\text{beam}} > m_{\tilde{\chi}_1^0} > m_{\tilde{e}_1} > m_{\tilde{\tau}_1}$), the following production processes are kinematically allowed

$$e^+e^- \rightarrow \tilde{\chi}_1^0 \tilde{\chi}_1^0 , \quad (1)$$

$$e^+e^- \rightarrow \tilde{e}_1^+ \tilde{e}_1^- , \quad \tilde{\mu}_1^+ \tilde{\mu}_1^- , \quad (2)$$

$$e^+e^- \rightarrow \tilde{\tau}_1^+ \tilde{\tau}_1^- . \quad (3)$$

The neutralino can decay to any of the sleptons:

$$\tilde{\chi}_1^0 \rightarrow e \tilde{e}_1 \rightarrow ee\tilde{G} , \quad (4)$$

$$\tilde{\chi}_1^0 \rightarrow \mu\tilde{\mu}_1 \rightarrow \mu\mu\tilde{G} , \quad (5)$$

$$\tilde{\chi}_1^0 \rightarrow \tau\tilde{\tau}_1 \rightarrow \tau\tau\tilde{G} . \quad (6)$$

Thus, the interesting final states in region I are $4e$, 4μ , 4τ , $2e2\mu$, $2e2\tau$ or $2\mu2\tau$ plus missing energy from the pair production of neutralinos.

In region II ($E_{\text{beam}} > m_{\tilde{e}_1} > m_{\tilde{\chi}_1^0} > m_{\tilde{\tau}_1}$), all the processes (1)–(3) are allowed. There are, however, additional final states because the selectron and smuon can decay into the neutralino first:

$$\tilde{e}_1 \rightarrow e\tilde{\chi}_1^0 \rightarrow e\tau\tilde{\tau}_1 \rightarrow e\tau\tau\tilde{G} , \quad (7)$$

$$\tilde{\mu}_1 \rightarrow \mu\tilde{\chi}_1^0 \rightarrow \mu\tau\tilde{\tau}_1 \rightarrow \mu\tau\tau\tilde{G} . \quad (8)$$

Given the choices the selectron or smuon will more likely decay through the $\tilde{\chi}_1^0$ because it involves the weak interaction whereas the direct decay to a lepton and a gravitino is gravitational. For the same reason the $\tilde{\chi}_1^0$ will decay to lepton-slepton rather than $\gamma + \tilde{G}$. Thus, the interesting final states are 4τ plus missing energy from process (1) or 6 charged leptons, four of which are taus, plus missing energy from process (2).

In region III ($m_{\tilde{e}_1} > E_{\text{beam}} > m_{\tilde{\chi}_1^0} > m_{\tilde{\tau}_1}$), only the processes (1) and (3) are kinematically allowed. The only allowed decays are

$$\tilde{\chi}_1^0 \rightarrow \tau\tilde{\tau}_1 \rightarrow \tau\tau\tilde{G} , \quad (9)$$

$$\tilde{\tau}_1 \rightarrow \tau\tilde{G} , \quad (10)$$

and so the final states are 4τ or 2τ with missing energy.

The cross-sections for the processes (1)–(3) are different. Usually the neutralino pair production cross-section is the largest of the three processes. Selectron pair production involves the s -channel γ and Z exchanges and the t -channel neutralino exchange while smuon and stau pair production involves only the s -channel γ and Z exchanges. So the production rate of a 6 lepton final state with 2 muons and 4 taus is in general different from that with 2 electrons and 4 taus. For an illustration of the relative magnitudes we show all these pair production cross-sections in Table 1 for four different scenarios.

In order that the signatures considered above be seen we assume that the decay length of the NLSP, $\tilde{\tau}_1$, into the τ -lepton and the gravitino is less than the size of the detector. If the decay length is significantly larger than the dimension of the detector, the $\tilde{\tau}_1$ will travel through the detector and be seen as a heavy charged particle. So, for example, rather than seeing four τ -leptons with missing energy, the signal would be two τ -leptons and two heavy charged particles without any missing energy. The decay width Γ for $\tilde{\tau}_1$ to $\tau\tilde{G}$ is

$$\Gamma = \frac{M_{\tilde{\tau}_1}^5}{16\pi F^2} \quad (11)$$

where \sqrt{F} is the SUSY breaking scale. The probability that a particle can travel a distance x before it decays is $P(x) = 1 - \exp^{-x/L}$, where L is the decay length given by [9,18]

$$L = (2 \times 10^{-16} \text{m}) \left(\frac{1 \text{ GeV}}{\Gamma} \right) \sqrt{\frac{E_{\tilde{\tau}_1}^2}{m_{\tilde{\tau}_1}^2} - 1} . \quad (12)$$

The last factor is the Lorentz factor. At LEPII, the energy $E_{\tilde{\tau}_1}$ of the scalar tau is only 1–2 times its mass, and so the Lorentz factor is only of order 1. To set a criterion for the $\tilde{\tau}_1$ to decay within the detector, we require $L \lesssim 2 \text{ m}$, which gives a condition on Γ :

$$\Gamma \gtrsim 10^{-16} \text{ GeV} . \quad (13)$$

Assuming $M_{\tilde{\tau}_1} \simeq 50 \text{ GeV}$, the condition $\Gamma \gtrsim 10^{-16} \text{ GeV}$ implies

$$\sqrt{F} \lesssim 5 \times 10^5 \text{ GeV} . \quad (14)$$

In summary, if $\sqrt{F} \gtrsim 5 \times 10^5 \text{ GeV}$ the decay of the $\tilde{\tau}_1$ is likely to be outside the detector; otherwise if $\sqrt{F} \lesssim 5 \times 10^5 \text{ GeV}$ the decay is within the detector. If $F_s \sim F$, then, this leads to the condition $\Lambda \gtrsim \sqrt{\frac{\lambda}{M/\Lambda}} 500 \text{ TeV}$ for the decay to take place outside the detector, where λ is the coupling by which the superfield S is coupled to the messenger fields. Similarly for smaller masses of selectrons and smuons the decays into $e\tilde{G}$ and $\mu\tilde{G}$ (Eq. (4) and Eq. (5)) can also happen outside the detector. In all these situation there would be two track of heavy charged particles instead of high p_T leptons in the final state.

IV. GMSB PARAMETER SPACE FOR THE REGIONS I, II AND II

In this section, we describe in detail our investigation of the GMSB parameter space that gives regions I, II, and III and of how probable these regions are. As mentioned before, the GMSB parameters are $M, \Lambda, n, \tan \beta$ and $\text{sign}(\mu)$. We take $\text{sign}(\mu)$ to be negative in order to satisfy the $b \rightarrow s\gamma$ constraint and vary n from 1 to 4, $\tan \beta$ from 1 to 50, and Λ from 10 TeV to 100 TeV. The value of M/Λ is restricted to the range 1.1 to 10^3 . We also impose the experimental constraints $m_h > 60$ GeV (where h is the lighter neutral scalar Higgs boson), $m_{\tilde{g}} > 200$ GeV (where \tilde{g} is the gluino), and $m_{\tilde{\tau}_1} > 45$ GeV. We summarize our results in the Λ - $\tan \beta$ plane for several values of n and M/Λ . Figures 1(a)–1(d) are for $\sqrt{s} = 172$ GeV, Fig. 2(a)–2(c) for $\sqrt{s} = 183$ GeV, and Fig. 3(a)–3(c) for $\sqrt{s} = 194$ GeV. In Fig. 1(a), we have used $n = 1$ and $M = 1.1\Lambda$. The curve $r \equiv m_{\tilde{\tau}_1}/m_{\tilde{\chi}_1^0} = 1$ corresponds to where the $m_{\tilde{\tau}_1} = m_{\tilde{\chi}_1^0}$. The region above this curve is for $\tilde{\tau}_1$ as the NLSP and we are primarily interested in this region. The darkest shaded region is excluded by the lighter neutral scalar Higgs boson mass $m_h < 60$ GeV. We also draw the contour of $m_{\tilde{g}} = 200$ GeV, to the left of which is also excluded. However, the most severe constraint comes from the demand that the stau mass to be greater than 45 GeV. The region on the right of the curve satisfies the constraint, as indicated by the arrow. The solid line labelled “neutralino= $E/2$ ” represents the contour along which $m_{\tilde{\chi}_1^0}$ is equal to the beam energy (which in this case is $E_{\text{beam}} = E/2 = 86$ GeV). The allowed region for $\tilde{\chi}_1^0$ -pair production is on the left of this contour. Another solid line labelled “selectron= $E/2$ ” corresponds to the contour along which $m_{\tilde{e}_R} = E/2$. This line separates region II from region III. The available regions at this energy are labelled II and III, as shown. There is no region I in this case. We see that there is a considerable range of $\Lambda \simeq 35 - 57$ TeV and $\tan \beta \simeq 18 - 34$ for which regions II and III are allowed. When the ratio M/Λ increases, the selectron and stau masses increase because of the increase in the threshold function $f(\Lambda/M)$; while the neutralino mass decreases due to the decrease in the threshold function $g(\Lambda/M)$. Consequently, region III would enlarge while region II would shrink. On the other hand, as $m_{\tilde{\chi}_1^0}$ decreases in order for $m_{\tilde{\tau}_1}$ to remain

the NLSP, larger values of $\tan\beta$ is needed. Thus the net result for the allowed region is an increase in the range of Λ but a decrease in the range of $\tan\beta$. In Fig. 1(a), we also show the cross-section contours for neutralino-pair production by the dashed lines. In regions II and III, the cross section varies from 0.05 pb to 0.65 pb. As Λ decreases the cross section first increases to a maximum and then decreases. This observation can be understood in terms of the two masses $m_{\tilde{\chi}_1^0}$, $m_{\tilde{e}_R}$ and the neutralino-mixing matrix element N_{11} . The cross section is roughly proportional to $|N_{11}|^4$. The smaller the Λ , the smaller the masses $m_{\tilde{\chi}_1^0}$ and $m_{\tilde{e}_R}$ will be, which give more phase space to the process $e^+e^- \rightarrow \tilde{\chi}_1^0\tilde{\chi}_1^0$, and so the cross section will increase. However, as Λ decreases the nature of the lightest neutralino changes from more gaugino-like to more higgsino-like, which causes a decrease in N_{11} . Consequently, the combined effect makes the cross section increase to a maximum when Λ decreases from a very large value. After this maximum the cross section decreases as Λ decreases further.

Next we consider Fig. 1(b). Here we show the effect of changing n to 2 but keeping M/Λ and \sqrt{s} the same as in Fig. 1(a). The available regions in this case are II and I but not region III. The reason for this change is that the increase in n causes the neutralino mass $m_{\tilde{\chi}_1^0}$ to increase more than the selectron mass $m_{\tilde{e}_R}$. The cross sections are somewhat smaller (~ 0.1 to 0.3 pb) in the available regions. When the ratio M/Λ is increased to 100, region I disappears but region III appears again for the reason mentioned above, as shown in Fig. 1(c). Note that the cross sections are larger here because in this case of $M/\Lambda = 100$, the matrix element $|N_{11}|$ decreases much less rapidly than that in the case of $M/\Lambda = 1.1$ when Λ decreases. It therefore implies that the cross section can increase to a higher maximum in this case of $M/\Lambda = 100$ when Λ decreases. In Fig. 1(d), we show the effect of increasing n to 4. It is clear that the available regions appear at smaller Λ and lower $\tan\beta$. We show regions I, II, and III and the cross sections for $E_{CM} = \sqrt{s} = 183$ GeV in Fig. 2 and those for $\sqrt{s} = 194$ GeV in Fig. 3.

We have shown in Figs. 1–3 the allowed regions I, II, and III in the Λ - $\tan\beta$ plane and cross sections for $e^+e^- \rightarrow \tilde{\chi}_1^0\tilde{\chi}_1^0$ within these regions. Failure to find the unique signals of this cross-section to some level would further restrict the Λ - $\tan\beta$ parameters. But what do

these restrictions mean in terms of more physical parameters such as the masses? Figures 1–3 show that $m_{\tilde{\chi}_1^0}$ and $m_{\tilde{e}_R}$ are roughly independent of $\tan\beta$ while $m_{\tilde{\tau}_1}$ is definitely not. For any one of choices of n and M/Λ a plot of $m_{\tilde{e}_R}$ as a function of $m_{\tilde{\chi}_1^0}$ is a unique line where $m_{\tilde{\tau}_1}$ depends on $\tan\beta$, as shown in Fig. 4(a). The intersection of the selectron line with the diagonal separates region I ($m_{\tilde{\chi}_1^0} > m_{\tilde{e}_R}$) from region II ($m_{\tilde{\chi}_1^0} < m_{\tilde{e}_R}$) while the intersection of stau with the diagonal bounds the lower end of region II since we always require $m_{\tilde{\tau}_1} < m_{\tilde{\chi}_1^0}$. The $\tan\beta = 20$ region is further bounded by the requirement that $m_{\tilde{\tau}_1}$ be larger than 45 GeV. These boundaries can then be applied to the cross-section as in Fig. 4(b). For example, for the n and M/Λ values used here, an experimental determination that the cross-section is less than 0.3 pb for $\sqrt{s} = 183$ GeV would rule out region II entirely and restrict $m_{\tilde{\chi}_1^0}$ to be larger than 73 GeV as can be seen from Fig. 4(b) or smaller than 65, 54, or 52 GeV for $\tan\beta$ equal 10, 15, or 20 as can be seen from Fig. 4(a). (In Fig. 4(b), the three cross section lines for each beam energy show the slight dependence of the cross section on $\tan\beta$.)

Figures 5(a) and 5(b) are similar to Figs. 4(a) and 4(b) but for $n = 2$ and $M/\Lambda = 100$ where region III is allowed but region I is not. The separation between regions II and III is fixed by the ratio of $m_{\tilde{e}_R}$ to the beam energy; the beam energy is taken as 97 GeV for the separation shown. The limit on the left side of region II is given by $m_{\tilde{\tau}_1} < m_{\tilde{\chi}_1^0}$ for $\tan\beta = 15$ but by $m_{\tilde{\tau}_1} > 45$ GeV for $\tan\beta = 20$ or 25. As before an upper bound on the cross-section can put limits on $m_{\tilde{\chi}_1^0}$. For example at $\sqrt{s} = 194$ GeV, an upper limit on the cross-section for the final states of region II of 0.6 pb implies $m_{\tilde{\chi}_1^0} > 67$ GeV or $m_{\tilde{\chi}_1^0} < 56$ GeV from Fig. 5(b) and from Fig. 5(a) $m_{\tilde{e}_R} > 82$ GeV or less than 74 GeV if $\tan\beta = 20$, but gives no constraint if $\tan\beta = 15$ or 25.

From the above results we conclude that there is a considerable region of the GMSB parameter space for which regions I, II, and III are available at LEPII energies. The production of the superparticles ($\tilde{\chi}_1^0, \tilde{e}_R, \tilde{\mu}_R, \tilde{\tau}_1$) in these available regions will give rise to the final states with two, four, or six charged leptons plus missing energy as discussed in section III. If such final states are not observed at LEPII, then the upper limit on the cross-section

times the branching ratios for these final states will further reduce the allowed regions, and will set new limits on the allowed masses for $\tilde{\chi}_1^0$, \tilde{e}_R , $\tilde{\mu}_R$ and $\tilde{\tau}_1$.

V. CHARGINO PAIR PRODUCTION AT LEPII

In the GMSB parameter space where $\tilde{\chi}_1^0$ is the NLSP, the chargino is always heavier than 100 GeV and, therefore, cannot be pair produced at LEPII [6]. On contrary, in the parameter space where the $\tilde{\tau}_1$ as the NLSP, there are regions in parameter space where the chargino is light enough to be pair produced at LEPII. In Figs. 6(a) and 6(b), we show the region in the Λ - $\tan\beta$ plane where the chargino mass is less than the beam energy for $n = 2$ and 4 with the experimental constraints as before. For $n = 2$ and $M/\Lambda = 1.1$, we get a triangular region around $\Lambda \simeq 20$ TeV and $\tan\beta \simeq 13 - 21$ as shown in Fig. 6(a). For $n=4$ the region expands somewhat around $\Lambda \simeq 13$ TeV and $\tan\beta \simeq 5 - 18$. Thus, there are regions in parameter space where not only the chargino mass is light enough to be pair produced at LEPII but also the other conditions are satisfied. The mass hierarchy in this region is

$$m_{\tilde{\chi}_2^0} \geq m_{\tilde{\chi}_1^\pm} > m_{\tilde{e}_1, \tilde{\mu}_1} > m_{\tilde{\chi}_1^0} > m_{\tilde{\tau}_1} . \quad (15)$$

The scalars \tilde{e}_1 and $\tilde{\mu}_1$ are essentially the right-handed selectron and smuon and have equal masses. The only allowed decay mode for the chargino is: $\tilde{\chi}_1^+ \rightarrow \nu_\tau \tilde{\tau}_1$: see table 2. (Since the lighter \tilde{e}_1 and $\tilde{\mu}_1$ are essentially right handed the branching ratios of the other two kinematically allowed decay modes, $\nu_e \tilde{e}_1$ and $\nu_\mu \tilde{\mu}_1$, are essentially zero.) The $\tilde{\tau}_1$ then decays to a τ -lepton and a gravitino with a 100% branching ratio. The final states arising from the decays of the produced chargino pair are two oppositely charged τ leptons, accompanied by large E_T . The corresponding background from the W -pair production is $\sigma \cdot B \sim 0.18$ pb, 0.21 pb, and 0.23 pb at the CM energies $\sqrt{s} = 172$ GeV, 183 GeV, and 194 GeV, respectively. In Table 2 we show the cross sections for chargino pair production at LEPII for some allowable scenarios. We see that the signal is considerably larger than the background.

VI. POLARIZED BEAMS

There is an interesting polarization effect present in the GMSB models. In these models, since the sparticles get their masses via gauge interactions, the masses of \tilde{e}_L and \tilde{e}_R are naturally split with \tilde{e}_R being much lighter than \tilde{e}_L . In supergravity models a large value of A or μ is needed in order to produce the same effect. This splitting has a significant effect on the cross section of $e^+e^- \rightarrow \tilde{\chi}_1^0\tilde{\chi}_1^0$ if a polarized electron beam is used. The dominant contribution to the cross section comes from the t -channel \tilde{e}_R exchange. Thus, with a right-handed polarized electron beam, the cross section will be much larger than with a left-handed polarized beam. A similar effect can be seen in the pair production of selectrons but the effect will be considerably smaller because selectron pair production also receives nonnegligible contributions from s -channel γ and Z exchanges. While these cross sections can change substantially by varying the beam polarization [25] in GMSB models, little change is expected in supergravity models. This technique can be used to distinguish between GMSB and supergravity models.

VII. CONCLUSION

In this work, we have studied in detail the parameter space in GMSB models where the $\tilde{\tau}_1$ is the NLSP. We have identified three regions in the Λ - $\tan\beta$ plane based on the mass hierarchies of the supersymmetric particles: $\tilde{\chi}_1^0$, \tilde{e}_R , and $\tilde{\tau}_1$. Different mass hierarchies produce different final states: 2 τ -leptons plus missing energy, 4 charged leptons plus missing energy, or six charged leptons plus missing energy. None of these signals involve hard photons. We have also calculated the contours of the cross sections for pair production of the lightest neutralinos in these regions for various LEPII energies. For practical purposes we have shown the same cross sections as a function of the neutralino mass. The cross section is in general of order 0.5 pb, which may be large enough to be observed at LEPII. The LEPII experiments should be able to find these SUSY signals or be able to rule out

part or all of these regions in the parameter space. Figures 1–5 summarize our findings.

In addition, we pointed out that there is a small region of parameter space where charginos may be light enough to be pair produced at LEPII. It gives clean signature of τ -leptons with large missing energy. We also pointed out that the cross section for $e^+e^- \rightarrow \tilde{\chi}_1^0\tilde{\chi}_1^0$ is sensitive to the electron beam polarization in GMSB models but not in supergravity models. A polarized electron beam can be employed to distinguish between these two supersymmetry breaking models.

ACKNOWLEDGEMENT

This work was supported in part by the US Department of Energy Grants No. DE-FG013-93ER40757, DE-FG02-94ER40852, DE-FG03-96ER-40969, and DE-FG03-91ER40674.

REFERENCES

- [1] M. Dine and A. Nelson, *Phy. Rev.* **D47**, 1277 (1993); M. Dine, A. Nelson and Y. Shirman, *Phys. Rev.* **D51**, 1362 (1995); M. Dine, A. Nelson, Y. Nir and Y. Shirman, *Phys. Rev.* **D53**, 2658 (1996); M. Dine, Y. Nir and Y. Shirman, preprint SCIPP-96-30, hep-ph/9607397.
- [2] I. Affleck, M. Dine and N. Seiberg, *Nucl. Phys.* **B256**, 557 (1997); R.N. Mohapatra and S. Nandi, *Phys. Rev. Lett.* **79**, 181 (1997); B. Dobrescu, *Phys. Lett.* **B 403**, 285,(1997); Z. Chacko, B. Dutta, R.N. Mohapatra and S. Nandi, hep-ph/9704307 (to be published in *Phys.Rev.D*).
- [3] S. Dimopoulos, M. Dine, S. Raby and S. Thomas, *Phys. Rev. Lett.* **76**, 3494 (1996); S. Ambrosanio, G. L. Kane, G. D. Kribs, S. P. Martin and S. Mrenna, *Phys. Rev. Lett.* **76**, 3498 (1996);
- [4] D. R. Stump, M. Wiest and C.P. Yuan, *Phys. Rev.* **D54**,1936, (1996).
- [5] K.S. Babu, C. Kolda and F. Wilczek, *Phys. Rev. Lett.* **77**, 3070, (1996).
- [6] S. Ambrosanio, G. L. Kane, G. D. Kribs, S. P. Martin and S. Mrenna, *Phys. Rev.* **D54**, 5395, (1996); *Phys. Rev.* **D55**, 1372, (1997).
- [7] S. Dimopoulos, S. Thomas and J.D. Wells, *Nucl. Phys.* **B488**, 39 (1997).
- [8] H. Baer, M. Brhlik, C.-H. Chen and X. Tata, *Phys. Rev.* **D56**, 4463 (1997).
- [9] J. Bagger, D. Pierce, K. Matchev and R.-J. Zhang, *Phys. Rev.* **D55**, 3188 (1997).
- [10] A. Riotto, O. Tornkvist and R.N. Mohapatra, *Phys. Lett.* **B 388**, 599 (1996).
- [11] G. Bhattacharyya and A. Romanino; *Phys. Rev.* **D55**, 7015 (1997).
- [12] K. Maki and S. Orito, hep-ph/9706382.
- [13] A. Datta, A. Kundu, B. Mukhopadhyaya and S. Roy, hep-ph/9707239.

- [14] Y. Nomura and K. Tobe, hep-ph/9708377.
- [15] B. Mukhopadhyaya and S. Roy, hep-ph/9709392 .
- [16] D. A. Dicus, B. Dutta and S. Nandi, Phys. Rev. Lett. **78**, 3055 (1997).
- [17] F. Borzumati, hep-ph/9702307.
- [18] S. Ambrosanio, G. Kribs and S. Martin, Phys. Rev. **D56**, 1761, (1997); hep-ph/9710217.
- [19] D. A. Dicus, B. Dutta and S. Nandi, hep-ph/9704225, (to appear in Phys. Rev. D).
- [20] B. Dutta and S. Nandi, hep-ph/9709511.
- [21] S. Dimopoulos, G.F. Giudice and A. Pomarol, Phys. Lett. **B389**, 37 (1996); S. P. Martin, Phys. Rev. **D55**, 3177 (1997).
- [22] V. Barger, M. Berger, P. Ohmann, and R. J. N. Phillips, Phys. Rev. **D51**, 2438 (1995), and references therein.
- [23] N. G. Deshpande, B. Dutta and S. Oh, Phys. Rev. **D56** 519 (1997); R. Rattazzi and U. Sarid , hep-ph/9612464.
- [24] H. Pagels and J. Primack, Phys. Rev. Lett. **48**, 223 (1982); T. Moroi et al., Phys. Lett. **B303**, 289 (1993).
- [25] This was first discussed by Dicus et. al in ref. [16]. See also ref. [15] where the detailed results for the cross-sections have been worked out.

TABLE CAPTIONS

Table 1 : Cross sections for $\tilde{\chi}_1^0 \tilde{\chi}_1^0$, $\tilde{\tau}_1^+ \tilde{\tau}_1^-$, $\tilde{e}_R^+ \tilde{e}_R^-$, and $\tilde{\mu}_R^+ \tilde{\mu}_R^-$ pair production at LEPII and the masses for the lightest neutralino $\tilde{\chi}_1^0$, lightest stau $\tilde{\tau}_1$, and the lightest selectron \tilde{e}_R in four different scenarios. The smuon and the selectron masses are the same.

Table 2 : Mass spectrum for the superpartners and $\tilde{\chi}_1^+ \tilde{\chi}_1^-$ pair production cross-sections at the LEPII for $\sqrt{s} = 172$, 183, and 194 GeV.

FIGURE CAPTIONS

Fig. 1: Regions I, II, and III and cross section contours (dashed lines) for $e^+e^- \rightarrow \tilde{\chi}_1^0 \tilde{\chi}_1^0$ at center-of-mass energy $E_{CM} = 172$ GeV in the Λ - $\tan\beta$ plane of the gauge-mediated models with experimental constraints from the lighter neutral Higgs boson, scalar tau, and gluino. The regions are defined by the mass hierarchy of the sparticle masses as follows: I: $E_{beam} > m_{\tilde{\chi}_1^0} > m_{\tilde{e}_R} > m_{\tilde{\tau}_1}$, II: $E_{beam} > m_{\tilde{e}_R} > m_{\tilde{\chi}_1^0} > m_{\tilde{\tau}_1}$, and III: $m_{\tilde{e}_R} > E_{beam} > m_{\tilde{\chi}_1^0} > m_{\tilde{\tau}_1}$. Above the contour $r \equiv m_{\tilde{\tau}_1}/m_{\tilde{\chi}_1^0} = 1$ the $\tilde{\tau}_1$ is the NLSP. The imposed constraints are: (i) the lighter neutral Higgs boson mass $m_h > 60$ GeV, the darkest shaded region is excluded, (ii) the gluino mass $m_{\tilde{g}} > 200$ GeV, the region on the right of the contour $m_{\tilde{g}} = 200$ GeV is allowed, and (iii) the stau mass $m_{\tilde{\tau}_1} > 45$ GeV, the allowed region is indicated by an arrow. In the figure, $E = E_{CM}$, (a) $n = 1, M = 1.1\Lambda$, (b) $n = 2, M = 1.1\Lambda$, (c) $n = 2, M = 100\Lambda$, and (d) $n = 4, M = 100\Lambda$

Fig. 2: Same as Fig. 1, except for $E_{CM} = 183$ GeV and we only show (a) $n = 1, M = 1.1\Lambda$, (b) $n = 2, M = 100\Lambda$, and (c) $n = 4, M = 100\Lambda$.

Fig. 3: Same as Fig.1, except for $E_{CM} = 194$ GeV and we only show (a) $n = 1, M = 1.1\Lambda$, (b) $n = 2, M = 100\Lambda$, and (c) $n = 4, M = 100\Lambda$.

Fig. 4: (a)The lighter selectron mass $m_{\tilde{e}_R}$ and the lighter stau mass $m_{\tilde{\tau}_1}$ versus the lightest neutralino mass $m_{\tilde{\chi}_1^0}$ for $n = 2, M = 1.1\Lambda$ at $E_{CM} = 194$ GeV. The selectron mass $m_{\tilde{e}_R}$

curve is roughly independent of $\tan\beta$ while the stau mass $m_{\tilde{\tau}_1}$ curves are shown for $\tan\beta = 10, 15, 20$. The upper boundary of region I is given by $m_{\tilde{\chi}_1^0} < E_{\text{beam}} = E_{CM}/2$. The separation between region I and II is determined by $m_{\tilde{e}_R} \leq m_{\tilde{\chi}_1^0}$. The lower boundary of region II is given by $m_{\tilde{\chi}_1^0} > m_{\tilde{\tau}_1}$ or $m_{\tilde{\tau}_1} > 45$ GeV, whichever gives a larger $m_{\tilde{\chi}_1^0}$, which is about 52, 54, and 65 GeV for $\tan\beta = 20, 15, 10$, respectively. Care has to be taken for smaller E_{CM} because the upper boundary of region I will shift towards smaller $m_{\tilde{\chi}_1^0}$. The diagonal straight line is $m_{\tilde{\tau}_1, \tilde{e}_R} = m_{\tilde{\chi}_1^0}$.

(b) Cross sections in pb for $e^+e^- \rightarrow \tilde{\chi}_1^0\tilde{\chi}_1^0$ at $E_{CM} = 172, 183$, and 194 GeV versus $m_{\tilde{\chi}_1^0}$ for $n = 2$ and $M = 1.1\Lambda$. The boundaries of regions I and II are the same as in part (a). The cross section has mild dependence on $\tan\beta$ and for each center-of-mass energy we show the cross section for $\tan\beta = 10$ (dot-dashed), 15 (solid), and 20 (dashed).

Fig. 5: Same as Fig. 4, but with $n = 2$, $M = 100\Lambda$, and regions II and III appears but not region I. The upper boundary of region III is given by $m_{\tilde{\chi}_1^0} < E_{\text{beam}}$. The separation between regions II and III are determined by $m_{\tilde{e}_R} \leq E_{\text{beam}}$. The lower boundary of region II is given by $m_{\tilde{\chi}_1^0} > m_{\tilde{\tau}_1}$ or $m_{\tilde{\tau}_1} > 45$ GeV, whichever gives a larger $m_{\tilde{\chi}_1^0}$, which is about 56, 68, and 74 GeV for $\tan\beta = 20, 15, 25$, respectively. Care has to be taken for smaller E_{CM} because the upper boundary of region III and the separation between II and III will both shift towards smaller $m_{\tilde{\chi}_1^0}$. The diagonal straight line is $m_{\tilde{\tau}_1, \tilde{e}_R} = m_{\tilde{\chi}_1^0}$.

Fig. 6: Figure showing the allowed region for chargino-pair production at LEPII with $\sqrt{s} = 183$ GeV for (a) $n = 2$, $M = 1.1\Lambda$ and (b) $n = 4$, $M = 1.1\Lambda$. The constraints shown are: $m_{\tilde{\tau}_1} > 45$ GeV, $r \equiv m_{\tilde{\tau}_1}/m_{\tilde{\chi}_1^0} < 1$, and $m_{\tilde{\chi}_1^+} < E/2$. Here $E = E_{CM}$.

Table 1

	Scenario 1	Scenario 2	Scenario 3	Scenario 4
	$\Lambda = 16 \text{ TeV},$ $n=3, M = 40\Lambda$ $\tan \beta = 16$	$\Lambda = 13 \text{ TeV},$ $n=4, M = 10\Lambda$ $\tan \beta = 15$	$\Lambda = 25 \text{ TeV},$ $n=2, M = 20\Lambda$ $\tan \beta = 20$	$\Lambda = 28 \text{ TeV},$ $n=2, M = 40\Lambda$ $\tan \beta = 18$
$M_{\tilde{\chi}_1^0}(\text{GeV})$	56	57	63	72
$m_{\tilde{\tau}_1}(\text{GeV})$	50	51	53	65
$m_{\tilde{e}_R}(\text{GeV})$	67	64	77	85
$\sqrt{s}=172 \text{ GeV}$				
$\sigma_{e^+e^- \rightarrow \tilde{\chi}_1^0 \tilde{\chi}_1^0}(\text{pb})$	0.65	0.43	0.59	0.33
$\sigma_{e^+e^- \rightarrow \tilde{\tau}_1^+ \tilde{\tau}_1^-}$	0.475	0.465	0.434	0.252
$\sigma_{e^+e^- \rightarrow \tilde{e}_R^+ \tilde{e}_R^-}$	0.246	0.165	0.103	0.003
$\sigma_{e^+e^- \rightarrow \tilde{\mu}_R^+ \tilde{\mu}_R^-}$	0.234	0.291	0.085	0.003
$\sqrt{s}=183 \text{ GeV}$				
$\sigma_{e^+e^- \rightarrow \tilde{\chi}_1^0 \tilde{\chi}_1^0}(\text{pb})$	0.68	0.45	0.65	0.43
$\sigma_{e^+e^- \rightarrow \tilde{\tau}_1^+ \tilde{\tau}_1^-}$	0.456	0.448	0.423	0.275
$\sigma_{e^+e^- \rightarrow \tilde{e}_R^+ \tilde{e}_R^-}$	0.326	0.212	0.191	0.052
$\sigma_{e^+e^- \rightarrow \tilde{\mu}_R^+ \tilde{\mu}_R^-}$	0.263	0.309	0.132	0.042
$\sqrt{s}=194 \text{ GeV}$				
$\sigma_{e^+e^- \rightarrow \tilde{\chi}_1^0 \tilde{\chi}_1^0}(\text{pb})$	0.70	0.46	0.70	0.52
$\sigma_{e^+e^- \rightarrow \tilde{\tau}_1^+ \tilde{\tau}_1^-}$	0.433	0.426	0.406	0.285
$\sigma_{e^+e^- \rightarrow \tilde{e}_R^+ \tilde{e}_R^-}$	0.396	0.254	0.277	0.118
$\sigma_{e^+e^- \rightarrow \tilde{\mu}_R^+ \tilde{\mu}_R^-}$	0.277	0.316	0.166	0.083

Table 2

	Scenario 1	Scenario 2	Scenario 3	Scenario 4
	$\Lambda = 13.5 \text{ TeV},$ $n=4, M = 1.1\Lambda$ $\tan \beta = 16$	$\Lambda = 17 \text{ TeV},$ $n=3, M = 1.1\Lambda$ $\tan \beta = 17$	$\Lambda = 20 \text{ TeV},$ $n=2, M = 80\Lambda$ $\tan \beta = 18$	$\Lambda = 22 \text{ TeV},$ $n=2, M = 3\Lambda$ $\tan \beta = 20$
$m_h(\text{GeV})$	111	111	107	110
m_{H^\pm}	153	160	199	183
m_A	130	115	182	165
$m_{\tilde{\chi}_1^0}$	59	59	48	51
$m_{\tilde{\chi}_2^0}$	112	107	84	88
$m_{\tilde{\chi}_3^0}$	119	129	182	161
$m_{\tilde{\chi}_4^0}$	225	215	212	203
$m_{\tilde{\chi}^\pm}$	82,225	85,216	80,214	82,204
$m_{\tilde{t}_{1,2}}$	57,120	56,123	46,128	50,132
$m_{\tilde{e}_{1,2}}$	64,117	66,11	68,119	69,124
$m_{\tilde{\nu}}$	84	88	88	94
$m_{\tilde{t}_{1,2}}$	404,458	405,457	326,401	386,439
$m_{\tilde{b}_{1,2}}$	403,416	403,418	334,359	384,405
$m_{\tilde{u}_{1,2}}$	407,416	408,418	348,360	395,406
$m_{\tilde{d}_{1,2}}$	408,423	410,426	350,369	395,413
$m_{\tilde{g}}$	609	554	356	397
μ	-105	-114	-167	-146
$\sigma_{e^+e^- \rightarrow \tilde{\chi}_1^+ \tilde{\chi}_1^-}(\text{pb})$				
$\sqrt{s} = 172 \text{ GeV}$	0.85	0.38	0.41	0.40
$\sqrt{s} = 183 \text{ GeV}$	1.02	0.68	0.50	0.50
$\sqrt{s} = 194 \text{ GeV}$	1.04	0.76	0.57	0.54

FIGURES

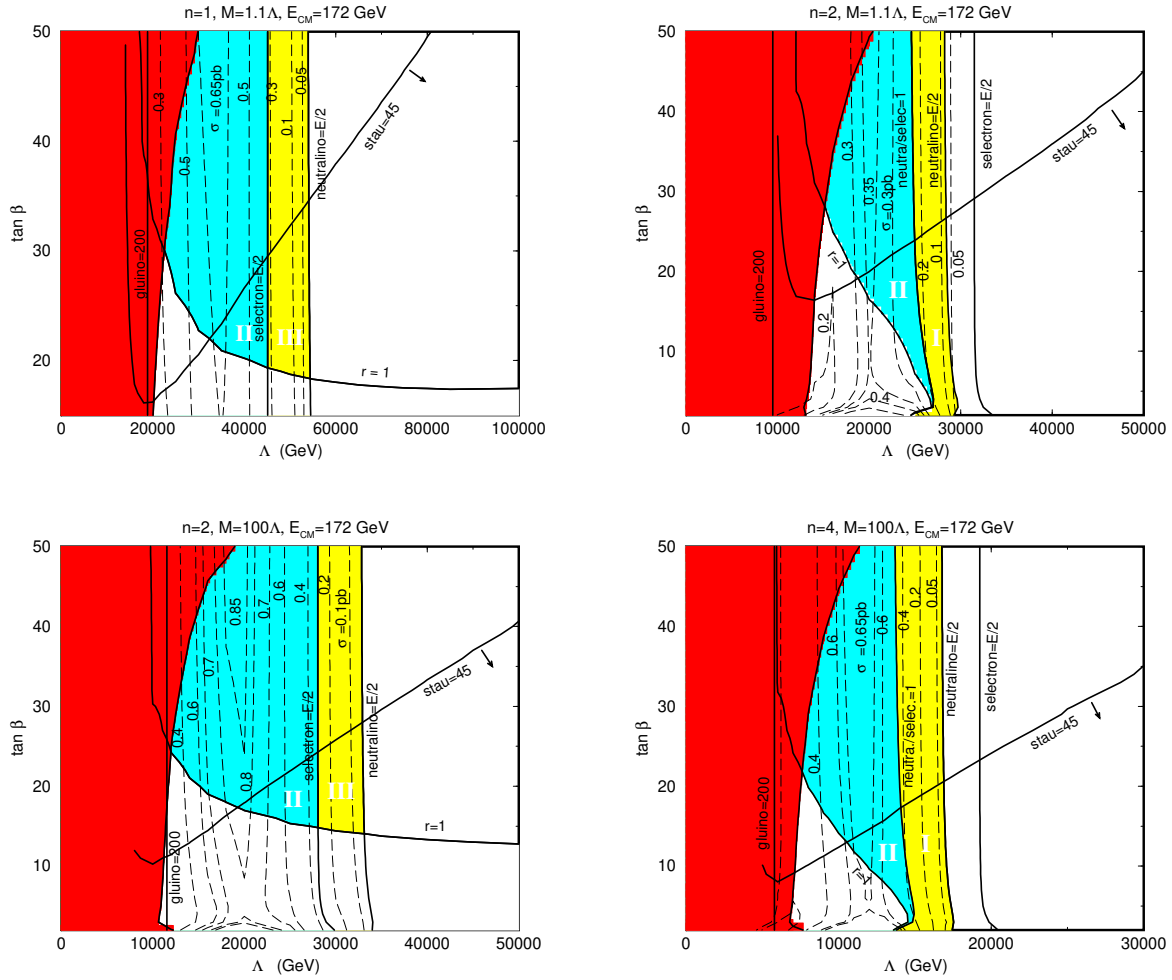


FIG. 1.

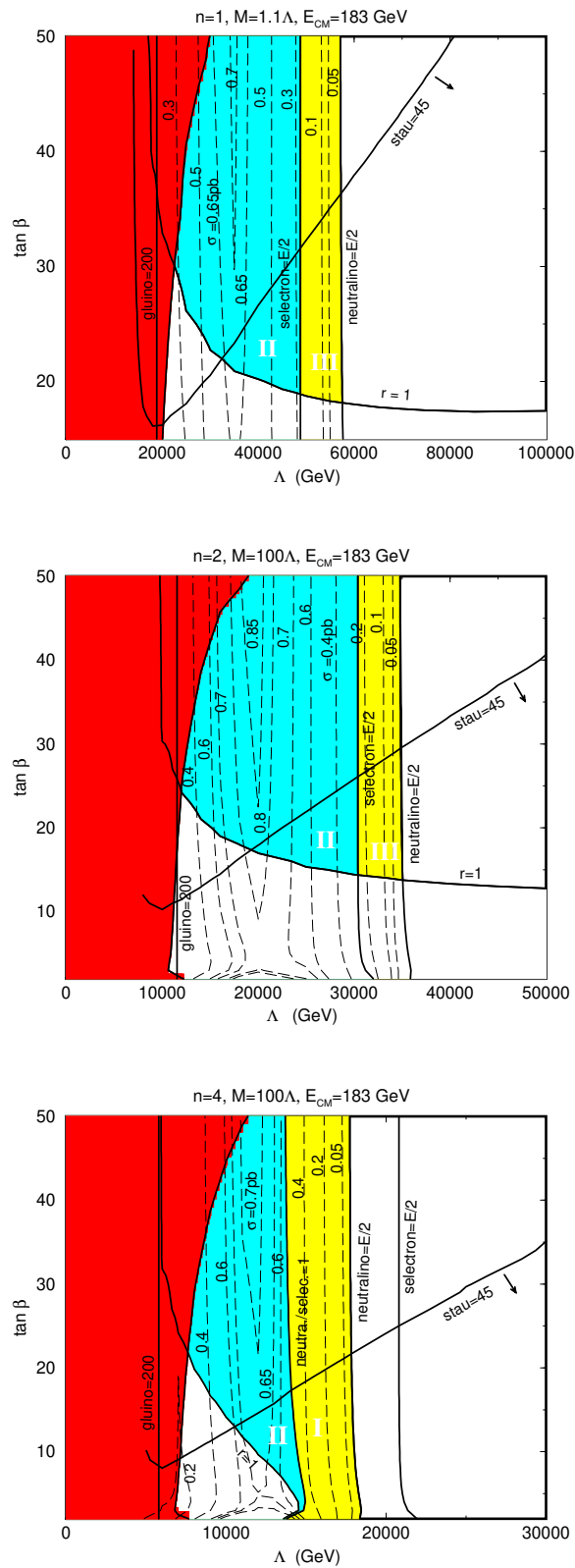


FIG. 2.

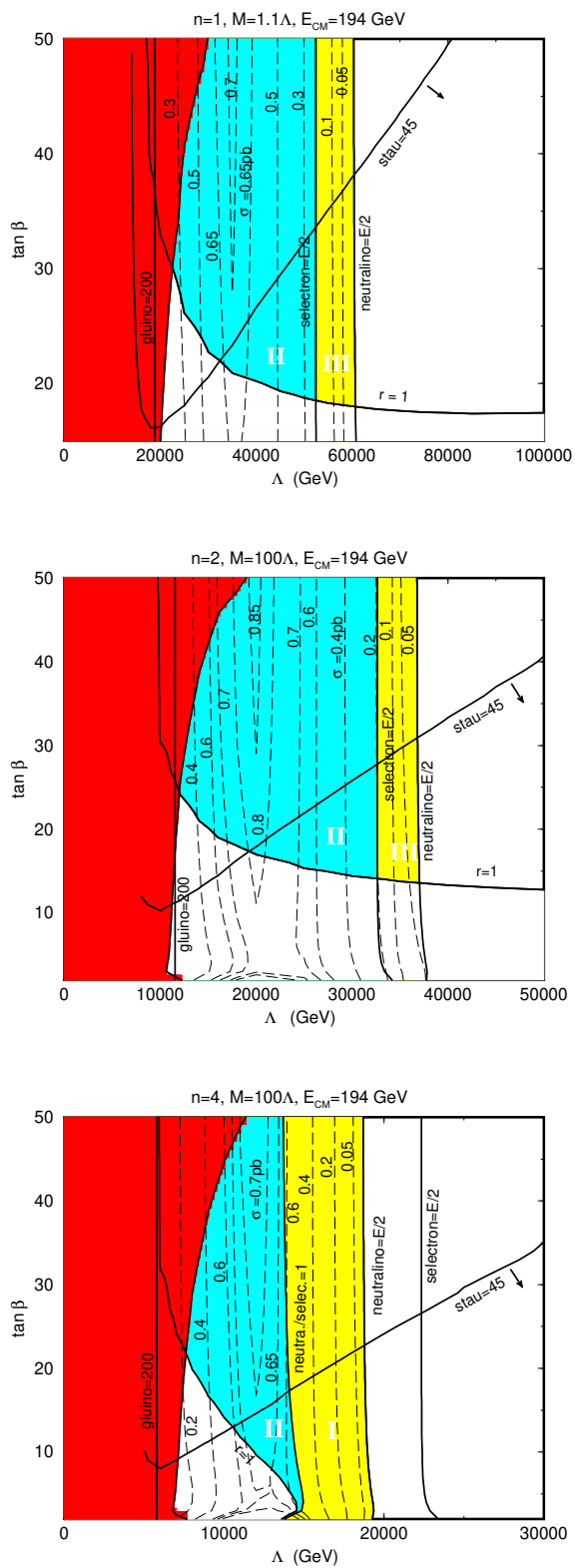


FIG. 3.

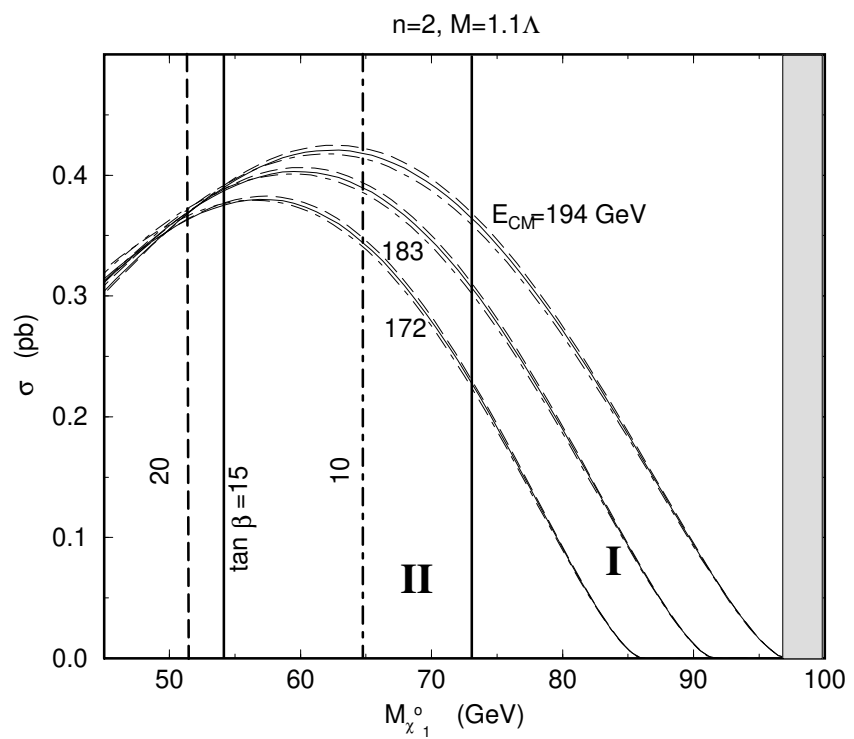
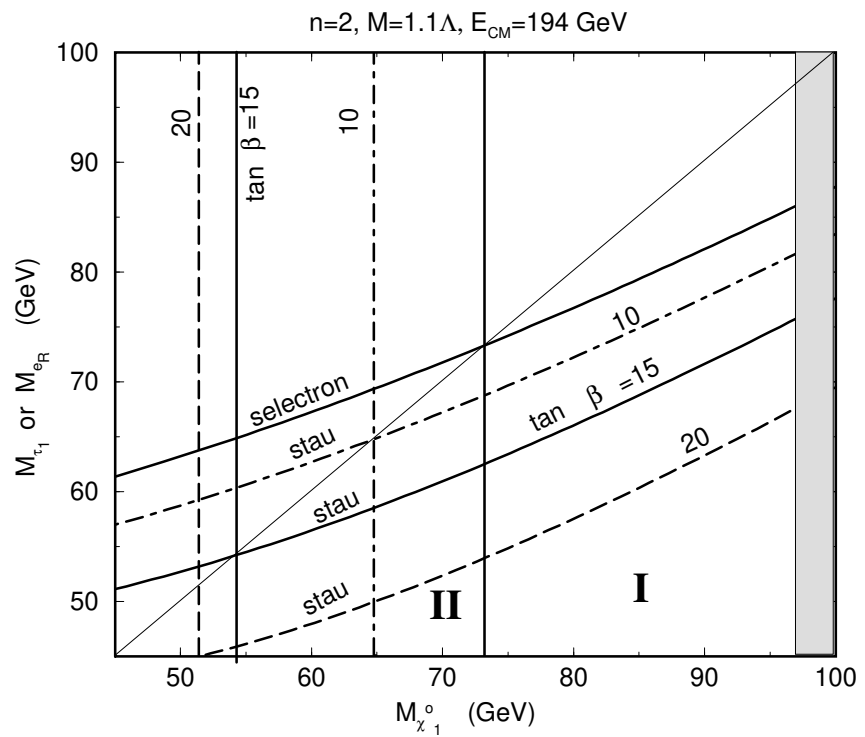


FIG. 4.

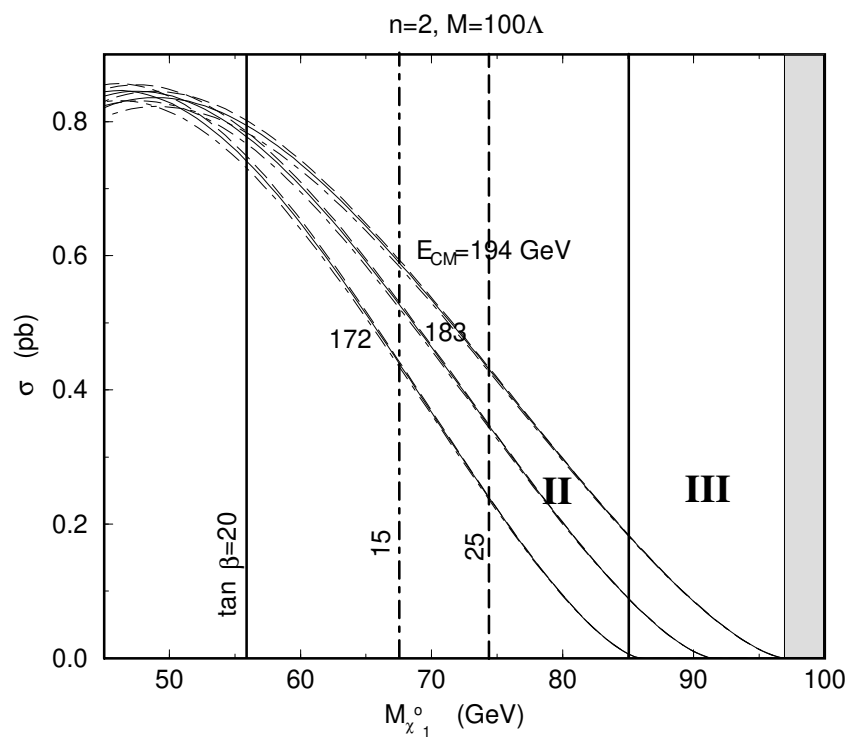
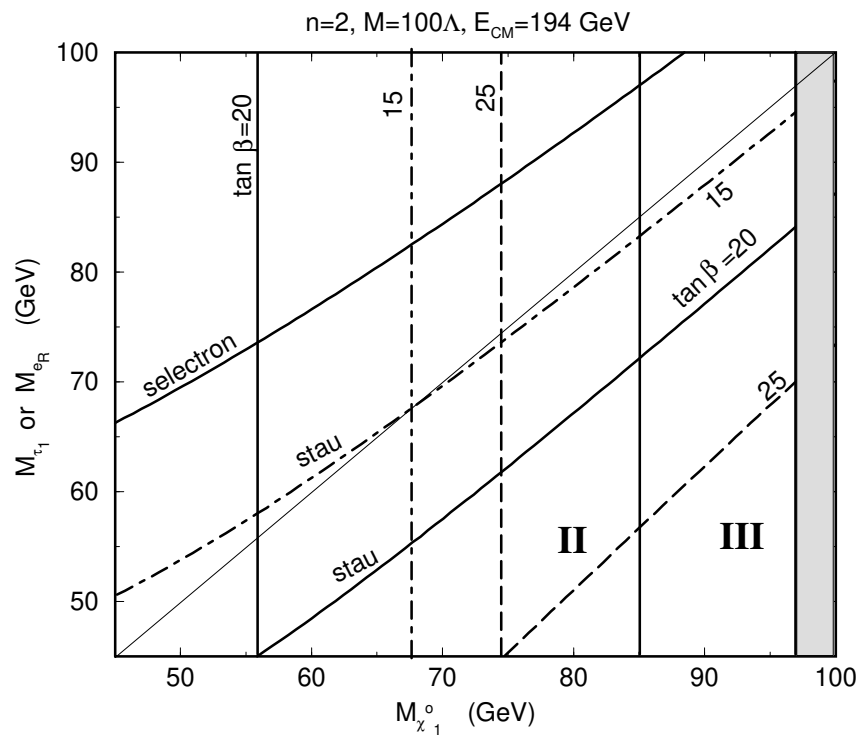


FIG. 5.

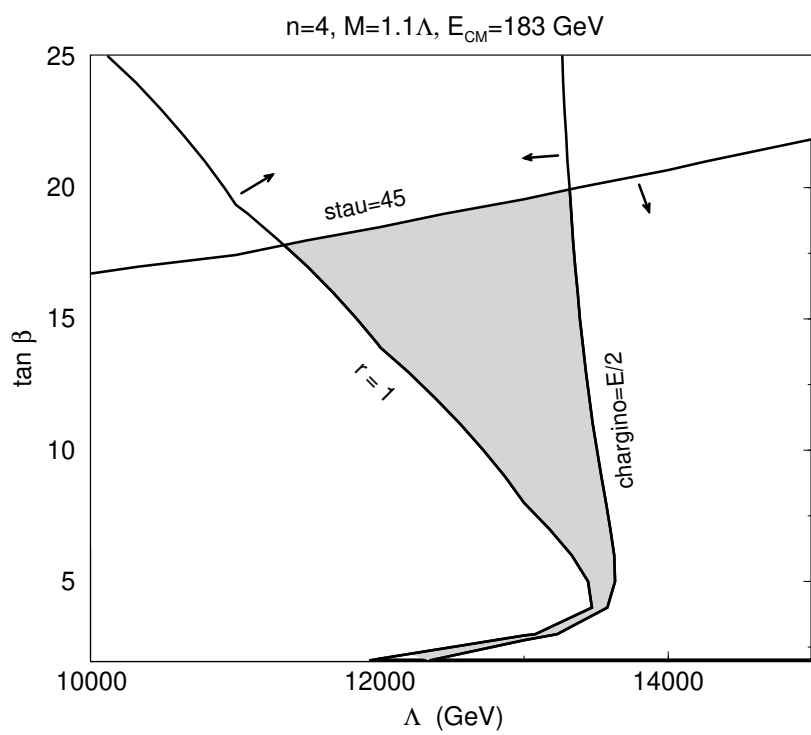
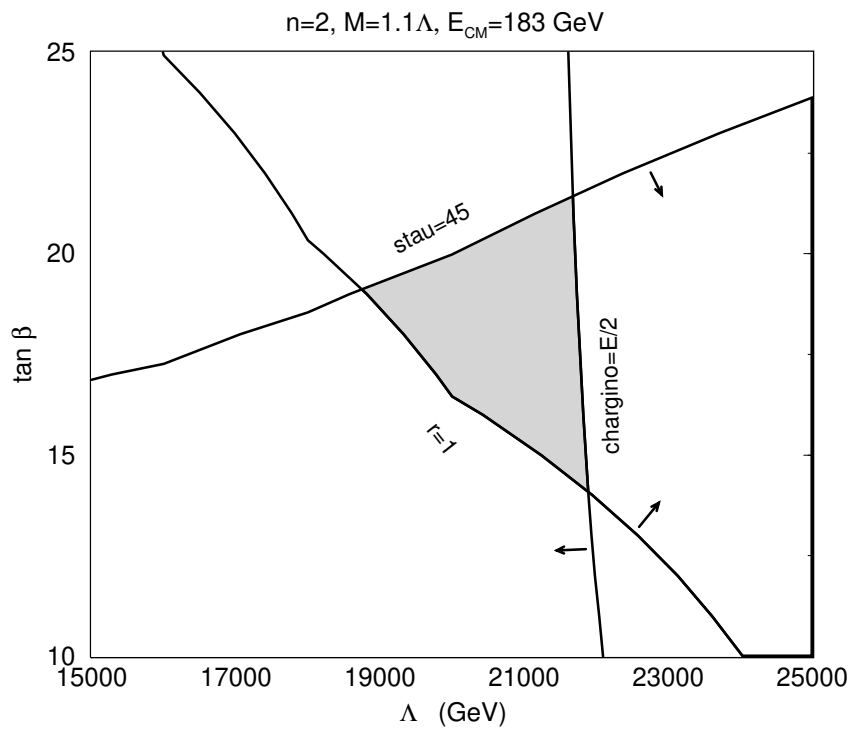


FIG. 6.